*Jordan Journal of Civil Engineering*, Volume **20**, No. **3**, **2026**
**DOI:** https://doi.org/10.14525/JJCE.v20i3.01

**Jordan Journal of Civil Engineering**

**Journal homepage:** https://jjce.just.edu.jo

# Durability Assessment of Waste-derived Mortar Binders in Marine and Sulphate-rich Environments: A Case of Glass Powder and Copper Slag

***Shruti Bhargava*** [1,2], ***P.V. Ramana*** [3], ***Kishan Lal Jain*** [4]*

[1] *Research Scholar, Department of Civil Engineering, Malaviya National Institute of Technology, Jaipur-302017, E-Mail: 2023rce9004@mnit.ac.in*
[2] *Assistant Professor, Arya College of Engineering, Jaipur, Rajasthan-302022, India.*
[3] *Associate Professor, Department of Civil Engineering, Malaviya National Institute of Technology, Jaipur-302017, India. E-Mail: pvramana.ce@mnit.ac.in*
[4] *Associate Professor, Department of Civil Engineering, Swami Keshvanand Institute of Technology, Management & Gramothan, Jaipur, Rajasthan-302017, India. * Corresponding Author. E-Mail: kishan.jain@skit.ac.in*

ARTICLE INFO

*Article History:*
Received: 20/4/2025
Accepted: 13/10/2025

ABSTRACT

This study explores the durability of eco-friendly mortar mixes incorporating copper slag (CS) and glass powder (GP) under aggressive environmental conditions. Glass powder was used to replace cement at 5%, 10%, 15%, 20%, and 25%, while copper slag replaced sand at 0% to 50% in 10% increments. Fixed cement to fine aggregate ratio of 1:4 was maintained throughout the study. The research focuses on evaluating the long-term performance of these modified mortars under aggressive exposure conditions, such as marine and sulphate-rich environments. Mechanical strength was assessed through compressive strength tests, while sustainability under harsh exposure conditions was evaluated using sulphate, acid resistance tests, carbonation depth analysis and rapid chloride penetration test (RCPT). The results demonstrated that optimal combinations, particularly those with 15%-20% GP and 30%-40% CS, significantly improved resistance to chemical attacks and reduced penetrability. Microstructural analysis using SEM and XRD confirmed the formation of additional C-S-H gel, denser internal structure, and reduced portlandite content, highlighting the pozzolanic contribution of GP and the filler effect of CS. The modifications enhanced durability and minimized deterioration, demonstrating the viability of GP and CS as sustainable alternatives for durable mortar incorporating industrial by-products.

***Keywords:*** Glass powder, Copper slag, Durability, Marine and sulphate-rich environments, Micro-structural analysis.

## INTRODUCTION

The growing emphasis on sustainable development in the construction industry has increased the focus on reusing industrial by-products to reduce environmental degradation and conserve natural resources. A wide range of industrial wastes—such as fly ash, waste glass, plastic and slag —have been utilized as alternative materials in mortar production (Hwang et al., 1998; A. Driouich et al., 2020; G. Ke et al., 2018; Jain et al., 2022). In India alone, over 62 million tonnes of waste are generated annually, underscoring the potential for resource recovery and reuse in infrastructure applications (Abukersh & Fairfield, 2011). One promising material in this domain is copper slag (CS), a by-product of copper manufacturing processes, with significant contributions from industries, such as Hindustan Copper Ltd. and Hindalco. Due to its stable

chemical composition and granular texture, CS has gained attention as a viable alternative to fine aggregates in cement-based materials (Bilir et al., 2015; Batis et al., 2015; Aouan et al., 2021). Casagrande et al. (2023) conducted a systematic review affirming that incorporating up to 40% CS can significantly enhance the mechanical properties of mortar, including flexural, compressive, and tensile strengths. Another extensively studied industrial waste is waste glass, which presents disposal challenges due to its non-biodegradable nature (Q. Li et al., 2022). Finely ground waste glass ash (WGA) is increasingly recognized as a promising sustainable supplementary cementitious material for use in mortar and concrete. Its pozzolanic nature promotes the formation of calcium silicate hydrate (C-S-H) gel during hydration, thereby enhancing the micro-structure and improving the long-term durability of cement-based composites (Ramadoss & Sundararajan, 2014). While waste glass used as coarse aggregate may induce alkali-silica reactions, leading to expansion and cracking (Jin & Chen, 2022), its finely ground form—waste glass powder (WGP)—exhibits pronounced pozzolanic properties. The multi-angular morphology of WGP also enables it to function as a micro-filler, refining the pore structure and resulting in a denser cement matrix (Casagrande et al., 2023; de Pedro et al., 2023). Studies have shown that replacing 20%-30% of cement with waste glass powder (WGP) can enhance compressive strength and resistance to chemical attacks. However, excessive replacement may reduce mechanical performance due to a lower cementitious content (Bilir, 2010; Sivasakthi, 2021; Saiz Martinez et al., 2017; Paul et al., 2025). Additionally, the synergy between copper slag (CS) and glass powder (GP) in cementitious composites has demonstrated significant potential. For example, Patel et al. (2021) found that mortars with 15% glass powder replacement exhibited slightly higher carbonation depth than control mixes, but their overall performance remained acceptable due to the denser micro-structure and reduced permeability. Ayub et al. (2024) observed that incorporating 10% GP in mortar containing CS as fine aggregate resulted in enhanced compressive strength, reduced shrinkage, and increased formation of calcium silicate hydrate gel. This denser micro-structure offers improved durability, particularly in aggressive environments. Studies by Xu et al. (2021) and Saranya et al. (2021) have specifically examined iron slag (or steel slag), which is notable for containing high-temperature minerals like dicalcium silicate ($C_2S$) and tricalcium silicate ($C_3S$), phases that are similar to those found in Portland cement. According to Sharma and Kaur (2020), replacing 30% of sand with copper slag and 15% of cement with glass powder reduced the total charge passed by up to 45%, indicating a significant improvement in chloride resistance. The fine particles in these materials contribute to pore refinement and increased densification of the matrix. In contrast to the pozzolanic behavior of copper slag, steel slag powder (SSP) is known for its latent hydraulic properties. However, a significant drawback of SSP is its slower hydration kinetics, which can lead to prolonged setting times and reduced early-age strength (Kou & Poon, 2020; Ramadoss & Sundararajan, 2014). A study by Singh et al. (2018) observed that mortar mixes incorporating 10%-20% glass powder exhibited lower strength loss and reduced surface erosion after prolonged acid exposure compared to control mixes. However, due to its rough texture and high surface area, copper slag (CS) enhances the bond between the cement and aggregate paste, thereby increasing the strength of concrete (Velumani et al., 2023). Research also indicate that CS aggregates can minimize metal leaching, ensuring environmentally safe construction (He et al., 2021; Arunchaitanya & Dey, 2023). Rao et al. (2019) found that mortars with 15% glass powder replacement showed up to 30% higher residual strength after 84 days in a sulphate solution compared to unmodified mortar. The denser micro-structure delayed the ingress of sulphate ions, reducing damage. Despite extensive studies on CS and glass powder (GP) individually, limited data exist on their combined use in mortars, particularly under sulphate-rich and marine conditions. The objective of this study is to bridge this gap by examining the durability and performance of mortars incorporating various proportions of glass powder (GP) and copper slag (CS). While both CS and GP are effective SCMs individually, their combination presents a synergistic opportunity to optimize performance. CS contributes significantly to the physical densification of the matrix and provides iron oxides, while GP offers a highly reactive source of amorphous silica. It is hypothesized that combining these materials may lead to a more balanced and efficient system. GP, with its high pozzolanic reactivity, could compensate for any potential reduction in early strength associated with CS. Conversely, the micro-filler effect of CS could

complement the pore-refining effect of GP, resulting in a composite matrix with superior mechanical properties and durability compared to systems containing a single SCM. The research will assess parameters, such as compressive strength, sulphate and acid resistance, carbonation depth, and rapid chloride permeability. Micro-structural analyses, including SEM and XRD, will provide a deeper understanding of the internal transformations and mechanisms influencing long-term performance.

## MATERIALS AND MIX CALCULATIONS

In this study, Zone II fine aggregate, as classified by IS 383:2016, was sourced from the Banas River. The physical characteristics of the fine aggregates are presented in Table 1. Copper slag was used as a partial replacement for natural river sand by weight of sand. Glass powder was sourced from soda-lime glass bottles, which were crushed, finely ground, and sieved through a 90-micron mesh to achieve a consistent particle size and enhance pozzolanic activity. Ordinary Portland Cement (OPC) of 43-grade, complying with IS 8112:2012 specifications, was used throughout the study. Both the physical and chemical properties of the cement were evaluated in the laboratory, and the corresponding data is included in Table 1. The particle size distribution curves of CS and sand are depicted in Figure 1. Micro-structural examination through Scanning Electron Microscopy (SEM) revealed notable morphological distinctions between the two materials. As shown in Figure 2, copper slag particles exhibited a rough and angular texture, which is expected to enhance mechanical interlocking within the concrete matrix. In contrast, river sand particles displayed smoother and more rounded surfaces. The chemical compositions of OPC, river sand, CS, and waste glass powder (WGP) were determined through X-ray Diffraction (XRD) analysis, the results of which are presented in Table 2. The XRD patterns shown in Figures 3(a) and 3(b) reveal a high content of quartz and alumina in both sand and copper slag. This mineralogical similarity supports the feasibility of using copper slag as an alternative to natural sand in cementitious materials.

**Table 1. Key index properties of cement, fine aggregate, copper slag, and glass powder**

| Property/ Parameter | Fineness Modulus (FM) | Specific Gravity | Water Absorption (%) | Bulk Density (g/cc) | Bulking of Fine Aggregate/ Zone | Soundness | Fineness | Consistency | Setting Time |
|---|---|---|---|---|---|---|---|---|---|
| **River Sand** | 2.82 | 2.66 | 15.4 | 1.585 | 20.20/ II | - | - | - | - |
| **Copper Slag** | 2.75 | 2.71 | 12.3 | 1.589 | 16.25/ II | - | - | - | - |
| **Glass Powder** | 0.91 | 2.53 | 0.80 | 2.586 | - | - | - | - | - |
| **Cement** | - | 3.07 | - | - | - | 2mm | 5% | 29% | 5hr. |

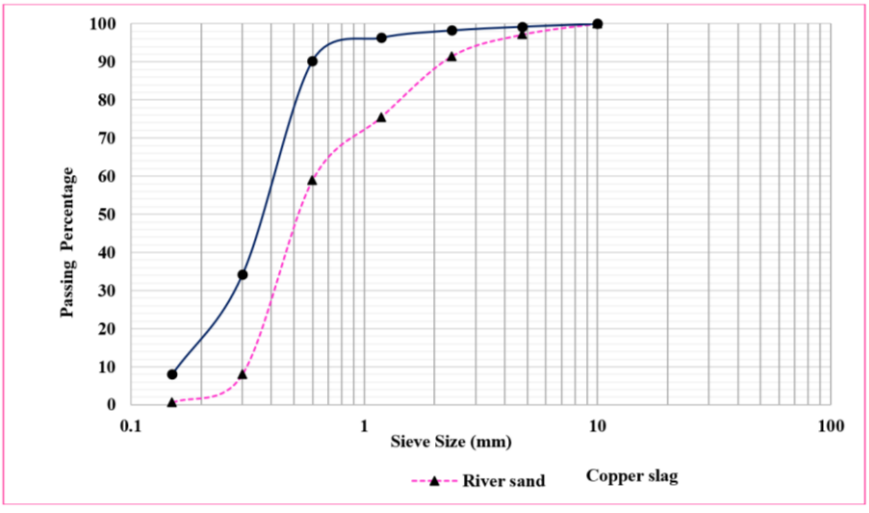


**Figure 1.** Particle size curves for sand and copper slag

**Table 2. Chemical compounds of mortar constitutes**

| Composition (%) | CaO | $SiO_2$ | $Al_2O_3$ | $Fe_2O_3$ | MgO | $SO_3$ | MnO | $Na_2O$ | $K_2O$ | $TiO_2$ | $P_2O_5$ | $H_2O$ |
|---|---|---|---|---|---|---|---|---|---|---|---|---|
| **Cement** | 64.9 | 21.00 | 4.2 | 2.3 | 1.5 | 1.7 | - | 0.33 | 0.45 | - | - | - |
| **Sand** | 3.45 | 72.23 | 10.75 | 3.60 | 1.29 | - | 0.05 | 2.30 | 1.91 | 0.43 | 0.10 | - |
| **CS** | 2.10 | 71.15 | 13.80 | 3.37 | 0.85 | - | 0.15 | 3.35 | 4.15 | 0.33 | 0.23 | 0.80 |
| **GP** | 9.8 | 73.00 | 0.35 | 0.28 | 3.08 | - | - | 13.79 | 0.16 | - | - | - |

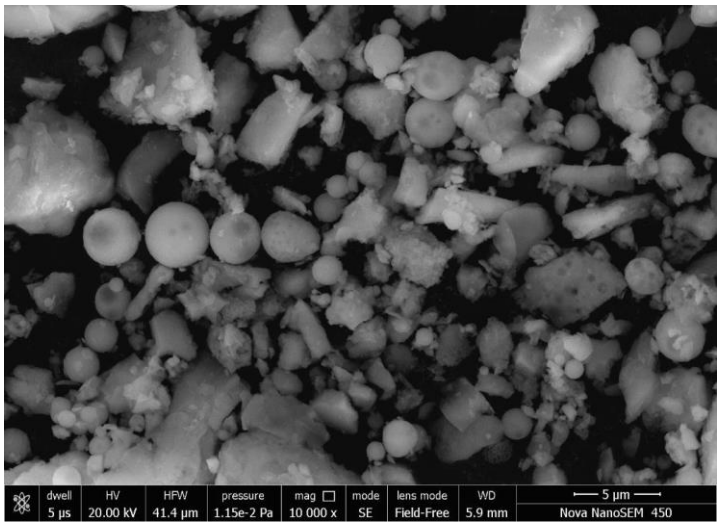


(a) SEM micrograph of cement

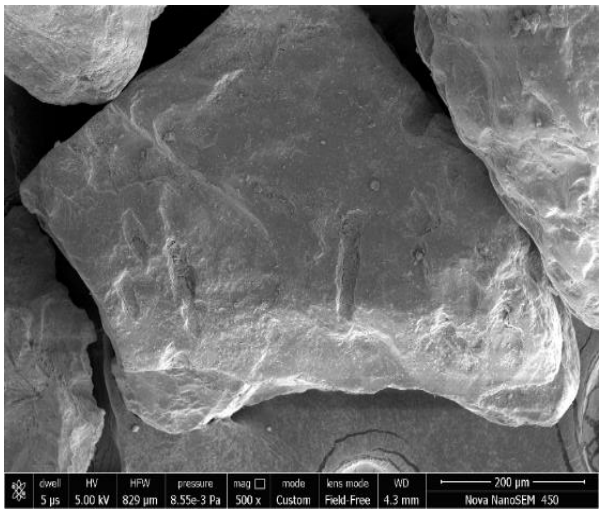


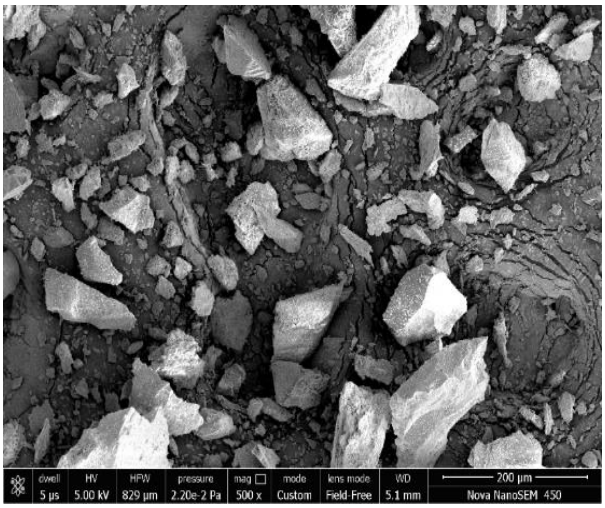


**Figure 2.** (b) SEM Image of sand (c) SEM image of copper slag

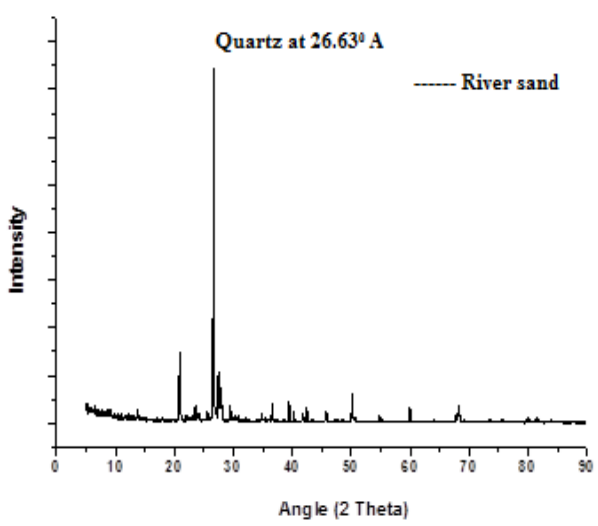


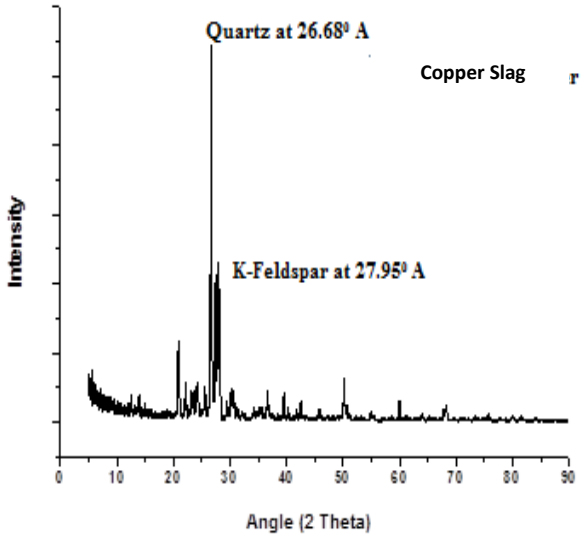


**Figure 3.** (a) XRD pattern for river sand (b) XRD pattern for copper slag

**Mix Calculations**

In this investigation, the cement-to-fine aggregate ratio for masonry mortar was maintained at 1:4 by weight. To determine the optimal water-to-cement (w/c) ratio corresponding to each level of material replacement, the flow table test was conducted in accordance with ASTM C1437-15. The objective was to ensure that the workability of the mortar—measured in terms of flow—remained within the desirable range of 105% to 115%. All mixes were prepared manually to reflect realistic field practices, and the calculated w/c ratios were carefully maintained for each mix to ensure consistency. The proportions of the individual constituents used per cubic meter of mix are detailed in Table 3.

**Table 3. Mix design details for 1 cubic meter of mortar**

| Percentage Replacement (%) | Cement (kg) | Glass Powder (kg) | Fine Aggregates | | Water (kg) | Water Binder Ratio |
|---|---|---|---|---|---|---|
| | | | Fine Aggregate (kg) | Copper Slag (kg) | | |
| **CM00** | 334.4 | 0 | 1336.2 | 0 | 307.7 | 0.92 |
| **CG0510** | 317.7 | 16.7 | 1202.6 | 133.6 | 296.2 | 0.89 |
| **CG1020** | 300.9 | 33.5 | 1068.9 | 267.2 | 284.6 | 0.85 |
| **CG1530** | 284.2 | 50.2 | 935.3 | 400.8 | 277.1 | 0.83 |
| **CG2040** | 267.5 | 66.9 | 801.7 | 534.5 | 269.6 | 0.81 |
| **CG2550** | 250.8 | 83.6 | 668.1 | 668.1 | 260.1 | 0.79 |

**CM00 =** Control mix.
**CG =** Copper slag and Glass powder GP=5, 10, 15, 20, and 25% CS=10, 20, 30, 40, and 50% (GP/CS; 5/10, 10/20, 15/30, 20/40 and 25/50).

## METHODOLOGY

**Compressive Strength**

The compressive strength of the mortar was evaluated following the guidelines specified in IS 4031 (Part 6):1988. Mortar cubes with dimensions of 50 mm× 50 mm × 50 mm were cast by placing the mix into molds in three equal layers. Each layer was compacted manually using 25 strokes of a tamping rod to ensure proper densification. To minimize air entrapment and achieve a smooth surface finish, the molds were then placed on a vibrating table. After 24 hours of setting, the cubes were demolded and placed in a water-curing tank. The specimens were cured for a total duration of 7, 28, 56, and

84 days, including the initial 24 hours. Compression tests were conducted using a calibrated compression testing machine at a certified laboratory, applying a uniform load at a rate between 2 N/mm² and 6 N/mm². Three specimens were tested for each mix variation to ensure accuracy and consistency of the results.

**Acid Attack Test Procedure**

To examine how acidic environments, affect mortar performance, specimens were immersed in a 5% sulfuric acid solution, following the durability testing procedures outlined in ASTM C267 (2001). To evaluate acid resistance, mortar cubes with dimensions of 70 mm × 70 mm × 70 mm and 50 mm × 50 mm × 50 mm were used. After moist curing, the specimens were immersed in the acidic medium for durations of 7-, 28-, 56-, and 84-day intervals. The resistance of the mortar mixes to acid attack was evaluated based on the changes in mass and compressive strength after exposure to an acidic environment, as shown in Figure 4. After curing, the initial mass and compressive strength of a set of control samples were recorded. The remaining specimens were then immersed in a 5% sulfuric acid ($H_2SO_4$) solution. The pH of the solution was monitored regularly and maintained constant throughout the exposure period of 84 days.

**Figure 4.** Mortar samples immersed in sulphuric acid solution

**Sulphate Attack Test Procedure**

To investigate the influence of sodium sulphate on mortar performance, specimens were submerged in a 5% sodium sulphate solution, in accordance with the ASTM C267 (2001) guidelines. Observations were made at 7, 28, 56, and 84 days to monitor variations in mass and compressive strength. Figure 5 shows the curing of mortar samples in sodium sulphate.

**Figure 5.** Mortar samples immersed in sodium sulphate

**Carbonation Test Procedure**

The carbonation resistance of mortar mixes was evaluated in accordance with the guidelines provided by RILEM CPC 18 (1988). Specimens measuring 40mm × 40mm × 160 mm were prepared, with all sides coated in epoxy paint except for one 40mm × 40 mm face, which was left exposed to facilitate controlled carbonation. The prepared specimens were exposed to a controlled carbonation environment, where the chamber conditions were maintained at 5% carbon dioxide concentration and 50% relative humidity. Carbonation depth measurements were taken after 7, 28, 56, and 84 days of exposure, as shown in Figure 6. At each interval, the specimens were split longitudinally, and a phenolphthalein solution was applied. The depth at which the color changed from pink to colorless was recorded as the depth of carbonation.


**Figure 6.** Specimen subjected to $CO_2$ in carbonation chamber

**Rapid Chloride Permeability Test (RCPT) Procedure**

To assess the durability characteristics of the mortar, the RCPT was carried out in accordance with ASTM C1202 (W, 2013). For this purpose, cylindrical samples measuring 100 mm in diameter and 50 mm in thickness were cast. The experimental setup involved placing the specimen between two compartments—one filled with a sodium hydroxide (NaOH) solution and the other with a sodium chloride (NaCl) solution. An electrical voltage was applied across the specimen to enable ionic movement. Six samples were tested simultaneously under uniform conditions. The current flowing through each sample was measured at 30-minute intervals over a total period of 600 minutes (10 hours). The total charge passed, expressed in Coulombs, was determined using the following formula. Figure 7 shows the arrangement of the RCPT test.

$$\textbf{Charge in Coulombs} = 900 \times [P_0 + (2 \times P_{30}) + (2 \times P_{60}) + (2 \times P_{90}) \ldots\ldots + (2 \times P_{600})]$$

where,

P = Current (in Amperes)

Abbreviation 0, 30, 60……..600 = Time period in minutes.

**Figure 7.** RCPT test setup

## RESULTS AND DISCUSSION

### Compressive Strength

The test results in Figure 8 show that the incorporation of GP and CS in the mortar mix leads to an increase in density. Among the tested samples, the mortar mix with (15% GP, 30% CS) replacement exhibited the highest average compressive strength, followed by the reference mortar mix. The reference mortar mix, without any GP and CS replacement, exhibited a lower average compressive strength compared to the (15% GP, 30% CS) mix. The superior performance of these mixes can be endorsed to the larger surface area of GP and CS particles, which increases water absorption. This reduces the water-binder ratio, ultimately leading to enhanced compressive strength (Ling, T.C et al., 2020). The 25% GP and 50% CS copper slag replacement mortar mix showed the lowest average compressive strength among the checked samples. This reduction in strength can be attributed to the inability to meet the designed water requirements at higher replacement levels, resulting in unhydrated binder particles (Shruti Bhargava at al., 2025). Consequently, this limits the formation of calcium silicate hydrate (CSH) gel, which is crucial for the development of compressive strength (Duan et al., 2020).

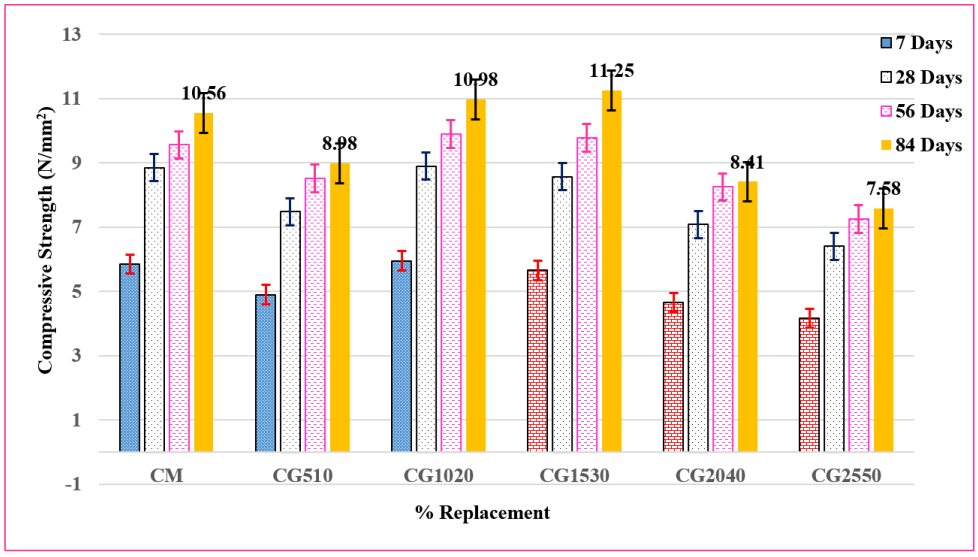


**Figure 8.** Test results of compressive strength

**Acid Attack**

Acid attack tests were conducted on 50 mm mortar cubes, with three specimens tested per exposure period. Substantial changes in compressive strength were observed between the GP+CS-modified mortars and the control specimens initially as shown in Figure 9. The compressive strength exhibited a significant decrease during the initial phase of acid exposure, primarily due to the rapid degradation of the surface matrix. However, the rate of strength loss gradually diminished over time, suggesting a slowing degradation process as the acid penetrated deeper into the specimens. This reduction was primarily due to the formation of soluble calcium salts, such as gypsum, which contributed to the weakening of the matrix. After 28 days, the development of expansive ettringite further exacerbated internal micro-cracking, significantly compromising the structural integrity of the specimens. By the end of 84 days, a sharp decrease in compressive strength—up to 45%—was observed. Gypsum began to deposit within the voids of the mortar matrix, thereby reducing the rate of weight loss up to 14 days of acid exposure for the 1:4 mixes (T. Wang et al., 2023). Over time, primary hydration products, like C-S-H and C-A-S-H, degrade, leading to the formation of secondary phases, such as basanite and expansive ettringite. These secondary products expand, weakening the matrix and causing increased disintegration, especially after 28 days of exposure. In the 1:4 mortar series, the strength loss ranged from 6.04% to 9.58%. Complete disintegration of the specimens was observed after 84 days of acid exposure, likely due to their lower cement content.

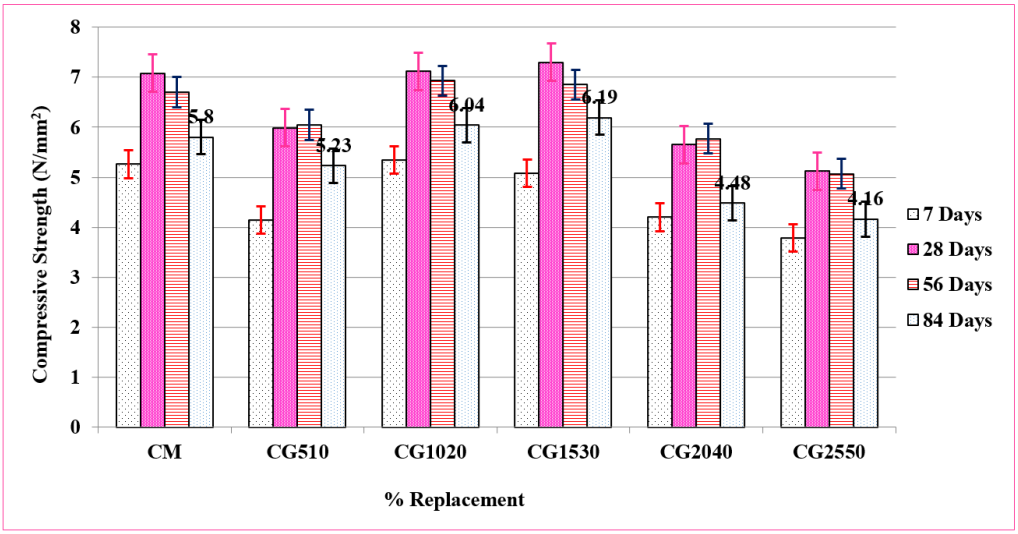


**Figure 9.** Test results of acid attack

**Sulphate Attack**

Figure 10 displays the residual compressive strength of mortar specimens following exposure to a sodium sulfate solution. The values shown are the average results from three mortar cubes, each measuring 50 mm. Across all mixes—whether incorporating glass powder (GP) and copper slag (CS) or not—there was no notable difference in compressive strength, regardless of the replacement ratios used. Interestingly, all mixtures exhibited a strength gain during the initial 84 days of sulfate exposure, with improvements ranging from 30% to 50% of their original strength. This reaction generates sodium hydroxide (NaOH), increasing the alkalinity of the pore solution. This highly alkaline environment is known to promote the stability and continued formation of strength-giving calcium silicate hydrate (C-S-H) gel. The resulting alkaline environment promoted the stabilization of key hydration compounds, such as calcium silicate hydrate (C-S-H), enhancing strength characteristics, as noted by Mehta and Monteiro (2006). The impact of sulfate attack was also evident in the observed weight loss of the specimens. Overall, the findings indicate that the addition of GP and CS did not compromise the mortar's resistance to sulfate-induced deterioration.

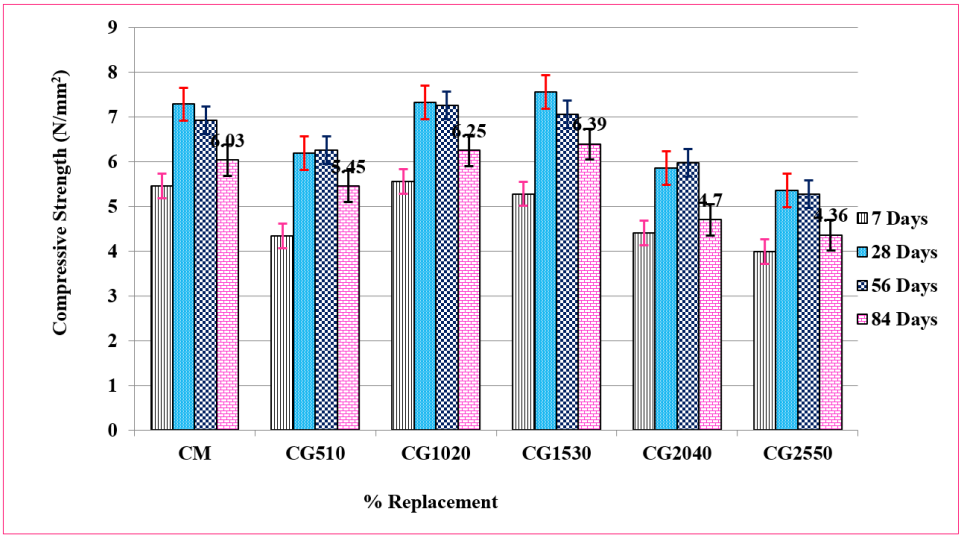


**Figure 10.** Test results of sulphate attack

**Carbonation**

Carbonation depth was evaluated after 7, 28, 56, and 84 days of exposure. At each interval, the specimens were split longitudinally, and phenolphthalein solution was applied to the freshly exposed surface to assess carbonation depth. The loss of pink coloration, indicating reduced alkalinity, was measured and is presented in Figure 11. The results indicate that the 1:4 GP+CS mortar mixes exhibited shallower carbonation depths compared to the control mix, suggesting improved resistance to $CO_2$ ingress. However, the variation among different mixes was not highly significant (Moghaddas et al., 2022). The chemical process occurring during carbonation is represented by the following reactions: carbon dioxide ($CO_2$) diffuses into the mortar and reacts with moisture ($H_2O$) to form carbonic acid ($H_2CO_3$). This weak acid reduces the alkalinity of the system, promoting the decomposition of portlandite [$Ca(OH)_2$] into calcium carbonate ($CaCO_3$). (P. Duan et al.,2016). The decrease in alkalinity leads to the observed color change from pink to colorless upon phenolphthalein application.

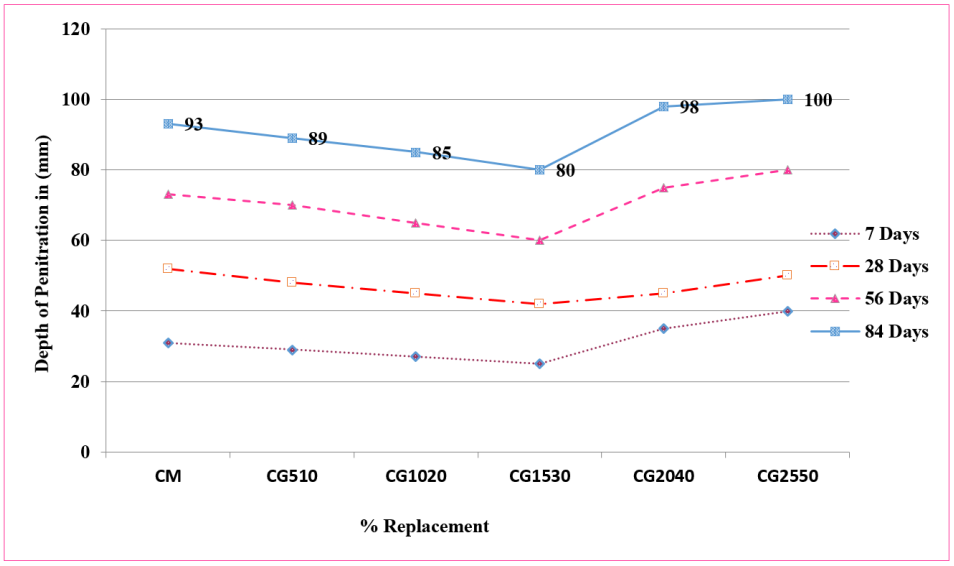


**Figure 11.** Depth of `carbonation

**RCPT Test Results**

RCPT test results for control and blended concretes are displayed in Figure 12. Results show that the value of minimum charge was observed for GP+CS/15+30

mix. The amount of charge calculated for control, GP+GS 0/0, GP+CS/10+20, GP+CS/15+30 and GP+CS/20+40 mixes, was 1925, 1524, 1417 and 2024 Coulombs, respectively. The observed reduction in the heat of hydration for mixes containing GP and CS is a direct result of their slower reactivity. The pozzolanic reaction of GP occurs after the primary cement hydration, leading to a lower and more extended heat release profile. Another reason was that extra C-S-H gel in concrete made it compact and dense, which restricted the charge to pass through it. Liu et al. (2018) also mentioned the same reason for reduction of charge and causes of low permeability. The increased charge passed observed in mixes with high GP and CS content is likely due to a less dense micro-structure. While the water-to-binder (w/b) ratio was kept constant, the high surface area and angular morphology of CS and GP may have increased the water demand. To maintain a consistent flow, a slight increase in the effective water content might have been necessary, which can lead to higher capillary porosity as the water evaporates. This increased porosity provides inter-connected pathways for ion migration, thereby increasing the permeability and the charge passed in the RCPT.

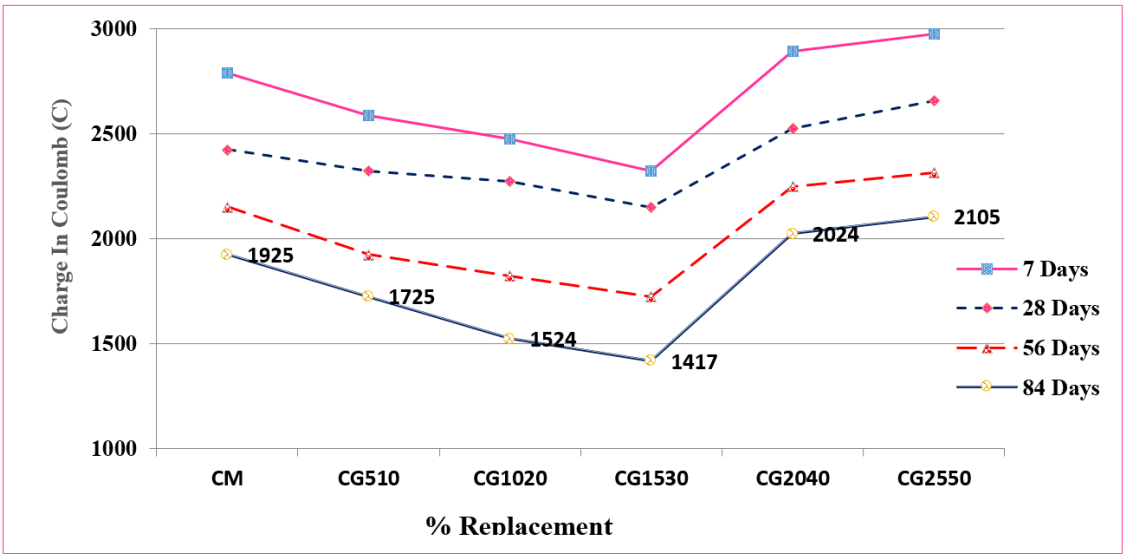


**Figure 12.** RCPT test results

**Scanning Electron Microscopy (SEM) Analysis**

SEM analysis was performed on various mortar specimens to assess the compactness and morphology of the micro-structure, influenced by the formation of hydration products. A representative portion of the hardened mortar was selected for analysis. The specimen was oven-dried to remove moisture which could interfere with imaging, and the surface was polished to ensure smoothness. To avoid charging effects during SEM analysis, the sample was coated with a thin conductive layer, such as gold or carbon, and then mounted onto an SEM stub using conductive adhesive. SEM micro-graphs of blended mortar mixes incorporating different proportions of glass powder and copper slag are shown in Figure 13(b). Mortar containing 15% GP and 30% CS exhibited a notably denser and more compact micro-structure than the control mix. This improvement is attributed to the finer particle size of GP and CS, which enhances particle packing and effectively fills voids within the matrix. The SEM image of the control sample may show a localized area with a high concentration of C-S-H gel. However, SEM provides a qualitative, two-dimensional view of a very small area, which may not be representative of the bulk micro-structure. Quantitative analysis through techniques, like XRD or MIP, would be required to compare total C-S-H content accurately. The improved mechanical and durability properties of the blended mixes strongly suggest that the secondary C-S-H formed from the GP reaction effectively refines the pore structure on a scale that is crucial for performance, even if it is not the dominant feature in a particular SEM micrograph (Ling et al., 2020). In contrast, is displays SEM images of mixes with higher replacement levels, where larger voids are apparent. This increased porosity is primarily due to insufficient calcium availability,

which limits the formation of C-S-H gel. Without adequate C–S–H, the bonding between filler particles is weakened, resulting in a more porous and mechanically inferior mortar structure (Saiz Martinez et al., 2017).

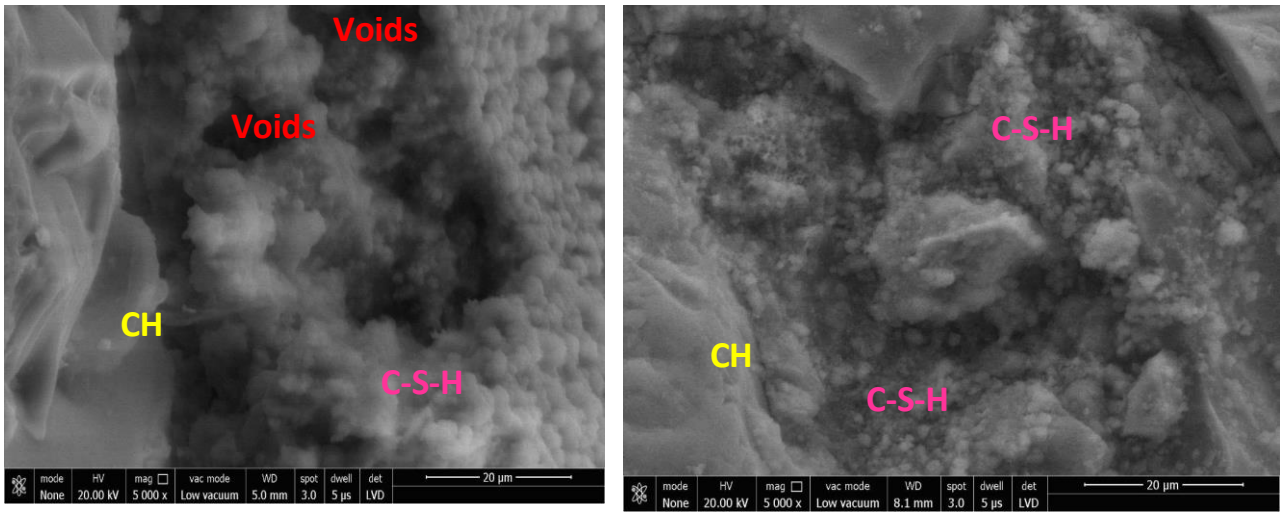


(a) Control Mix (b) CG1530 Mix

**Figure 13.** Images of SEM analysis

**X-ray Diffraction (XRD) Analysis**

The XRD test is used to identify crystalline segments in a material by analyzing the relative intensities of peaks within the diffraction pattern. For this test, an appropriate portion of hardened mortar is selected and finely ground—typically using a mortar and pestle or a mechanical grinder—until a uniform powder is obtained. The powder is then sieved to ensure a consistent particle size, generally below 75 microns. This fine powder is placed into a sample holder and compacted to form a smooth, level surface suitable for XRD analysis.As shown in Figure 14, the control mortar exhibited prominent calcium hydroxide (CH) peaks between 20° and 40° 2θ, indicating the presence of unreacted CH. However, with the incorporation of glass powder (GP), which provides additional reactive silica, much of this CH was converted into calcium-silicate-hydrate (C–S–H), as also noted by Ling et al. (2020). The GP-modified mixes displayed more pronounced C–S–H peaks in the 30° to 80° 2θ range, along with a noticeable reduction in CH peak intensity. These observations align with the mechanical and durability test results, further confirming the beneficial role of copper slag as a fine aggregate and glass powder as a partial cement replacement in enhancing the micro-structural properties of the mortar.

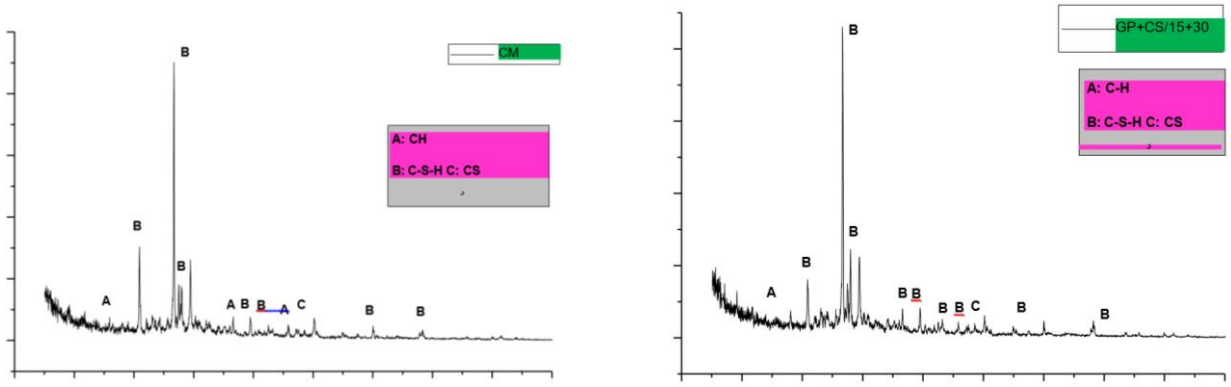


(a) Control Mortar (b) CG1530

**Figure 14.** Images of XRD analysis

## CONCLUSIONS

This study confirms the potential of copper slag (CS) and glass powder (GP) as sustainable partial replacements for fine aggregate and cement, respectively, in mortar formulations. Comprehensive testing was conducted including compressive strength, acid and sulphate resistance, carbonation depth, Rapid Chloride Penetration Test (RCPT), and micro-structural analyses (XRD and SEM). This study demonstrated that an optimal combination of 15% GP and 30% CS can produce mortar with performance characteristics equivalent or superior to conventional mortar, while utilizing a substantial volume of industrial by-products. The key finding is that this optimal mix consistently achieved performance metrics that were statistically equivalent to those of the control mix across all tests. In several key durability tests, such as acid and sulfate resistance, the (15% GP, 30% CS) mix showed a marked improvement. However, for certain properties, like early compressive strength, the observed average increase was not statistically significant when error bars (representing standard deviation) are considered. Mechanical properties, particularly compressive strength, improved notably at moderate replacement levels, while durability under chemical exposure (acid and sulphate) and carbonation conditions also showed better resistance.

- The maximum compressive strength was achieved with the mix containing 15% GP and 30% CS, showing a 9.38% increase over the control mix. Under acid and sulphate exposure, this mix also exhibited superior resistance, indicating improved durability.
- The minimum carbonation depth was observed in the same mix (15% GP and 30% CS), registering 16.25% less than that of the control, suggesting enhanced resistance to carbon dioxide ingress.
- RCPT results indicated reduced chloride ion permeability, contributing to improved long-term durability in aggressive environments.
- Micro-structural analysis confirmed a denser matrix in the optimized mixes, attributed to better particle packing and the formation of additional calcium-silicate-hydrate (C–S–H) gel due to pozzolanic activity.
- Overall, incorporating GP and CS at these optimal levels enhances both mechanical strength and durability, especially under aggressive environmental conditions, while also promoting environmentally sustainable construction.

**Acknowledgments**

The authors gratefully acknowledge the support provided by Swami Keshvanand Institute of Technology (SKIT), Jaipur; Malviya National Institute of Technology (MNIT), Jaipur; and Arya College of Engineering, Jaipur. The authors sincerely appreciate the research facilities and resources extended by SKIT and MNIT during the course of this study. Special thanks are due to the faculty and laboratory staff of the Civil Engineering Department for their valuable assistance and cooperation throughout the research work.

## REFERENCES

Aliabdo, A.A., Abd Elmoaty, A.E.M., & Aboshama, A.Y. (2016). Utilization of waste glass powder in the production of cement and concrete. *Construction and Building Materials, 124*, 866-877.

Al-Jabri, K.S., Al-Harthi, M.A., & Al-Saidy, A.H. (2006). Effect of copper slag as a fine aggregate on cement mortars and concrete properties. *Construction and Building Materials, 20*(8), 578-585. https://doi.org/10.1016/j.conbuildmat.2005.02.005

Aouan, B., Alehyen, S., Fadil, M., El Alouani, M., Khabbazi, A., Atbir, A., & Taibi, M. (2021). Compressive strength optimization of metakaolin-based geopolymer by central composite design. *Chemical Data Collections, 31*, 100636. https://doi.org/10.1016/j.cdc.2020.100636

ASTM International. (2001). *ASTM C267: Standard test methods for chemical resistance of mortars, grouts, and monolithic surfacings and polymer concretes.* ASTM International.

ASTM International. (2016). *ASTM C109M-16a: Standard test method for compressive strength of hydraulic cement mortar (Using 50-mm cube specimens).* ASTM International.

Babu, T., & Thangaraj, S. (2023). Eco-friendly geopolymer ternary mortar with GGBS, bagasse ash, and sewage sludge ash. *KSCE Journal of Civil Engineering, 27*, 3441-3454.

Batis, G., Pantazopoulou, P., Tsivilis, S., & Badogiannis,

E. (2005). The effect of metakaolin on the corrosion behavior of cement mortars. *Cement and Concrete Composites, 27*(1), 125-130.

Bhargava, S., Jain, K.L., Ramana, P.V., & Sharma, D.K. (2025). Durability and micro-structure of mortar with glass powder and copper slag. *Jordan Journal of Civil Engineering, 19*(2). https://doi.org/10.14525/JJCE.v19i2.01

Bilir, T., Gencel, O., & Topcu, I. B. (2015). Properties of mortars with fly ash as fine aggregate. *Construction and Building Materials, 93*, 782-789. https://doi.org/10.1016/j.conbuildmat.2015.05.021

Borhan, M.M., & Mohamed, S.N. (2022). *Laboratory study of water absorption of modified mortar.*

British Standards Institution. (2000). *BS 1015-12: Methods of test for mortar for masonry - Determination of adhesive strength of hardened rendering and plastering mortar on substrates.*

Bureau of Indian Standards. (1963). *IS 2386-3: Methods of test for aggregates for concrete - Specific gravity, density, voids, absorption, and bulking.*

Bureau of Indian Standards. (1998-2019). *IS 4031 series: Methods of physical tests for hydraulic cement.*

Bureau of Indian Standards. (2016). *IS 383: Natural coarse and fine aggregates for concrete & mortar.*

Casagrande, C.A. (2023). Copper slag in cementitious composites: A systematic review. *Journal of Building Engineering, 78*, 10725. https://doi.org/10.1016/j.jobe.2023.107725

Chandra Paul, S., Savija, B., & Babafemi, A.J. (2018). Mechanical and durability properties of cement composites with waste glass. *Journal of Cleaner Production, 198*, 891-906.

Christy, C.F., & Tensing, D. (2010). Effect of class-F fly ash as a partial replacement with cement and fine aggregate in mortar. *Indian Journal of Engineering and Materials Sciences, 17*, 140-144.

Deb, P.S., Nath, P., & Sarker, P.K. (2015). Drying shrinkage of slag-blended fly ash geopolymer cured at room temperature. *Procedia Engineering, 125*, 594-600.

Driouich, A., Chajri, F., El Hassani, S.E.A., Britel, O., Belouafa, S., Khabbazi, A., & Chaair, H. (2020). Optimization synthesis geopolymer based mixture metakaolin and fly ash activated by alkaline solution. *Journal of Non-Crystalline Solids, 544*, 120197. https://doi.org/10.1016/j.jnoncrysol.2020.120197

Duan, P., Yan, C., Luo, W., & Zhou, W. (2016). Nano-$TiO_2$ effects on geopolymer paste strength and shrinkage. *Construction and Building Materials, 106*, 115-125.

Fan, J., Yan, J., Zhou, M., Xu, Y., Lu, Y., Duan, P., Zhu, Y., Zhang, Z., Li, W., Wang, A., & Sun, D. (2023). Heavy metal immobilization of ternary geopolymer based on nickel slag, lithium slag, and metakaolin. *Journal of Hazardous Materials, 453*, 131380. https://doi.org/10.1016/j.jhazmat.2023.131380

Guo, Y., Xie, J., Zheng, W., & Li, J. (2018). Steel slag as fine aggregate in concrete. *Construction and Building Materials, 192*, 194-201.

Gupta, L.K., & Vyas, A.K. (2018). Impact on mechanical properties of cement fine aggregate mortar containing waste granite powder. *(Incomplete citation)*

He, P., Zhang, B., Lu, J.-X., & Poon, C.S. (2021). Reaction mechanisms of alkali-activated glass powder-GGBS-CAC composites. *Cement and Concrete Composites, 122*, 104143. https://doi.org/10.1016/j.cemconcomp.2021.104143

He, R., Zhang, S., Zhang, X., Zhang, Z., Zhao, Y., & Ding, H. (2021). Copper slag: Leaching behavior of heavy metals and applicability as supplementary cementitious material. *Journal of Environmental Chemical Engineering, 9*, 105132. https://doi.org/10.1016/j.jece.2021.105132

He, Z.-H., Han, X.-D., Zhang, M.-Y., Yuan, Q., Shi, J.-Y., & Zhan, P.-M. (2022). A novel development of green UHPC containing waste concrete powder. *Powder Technology, 398*, 117075.

Hwang, K.R., Noguchi, T., & T., T.F. (1998). Effect of fine aggregate replacement on rheology, compressive strength, and carbonation of fly ash mortar. *ACI Special Publication, SP-178*, 401-410.

Irki, I., Debieb, F., Quzadid, S., Larouci, H., Settari, C., & Boukhelkhel, D. (2023). Effect of blaine fineness of recycled brick powder replacing cementitious materials in self-compacting mortar.

Jain, K.L., Sharma, D.K., Choudhary, R., & Bhargava, S. (2023). Impact of waste iron slag on mechanical and durability properties of concrete. *Jordan Journal of Civil Engineering, 17*(1).

Jiang, Y., Ling, T.-C., Shi, C., & Pan, S.-Y. (2018). Characteristics of steel slags and their use in concrete: A review. *Resources, Conservation & Recycling, 136*, 187-197.

Jin, Q., & Chen, L. (2022). A review of the influence of copper slag on cement-based materials. *Materials, 15*(23), 8594. https://doi.org/10.3390/ma15238594

Ke, G., Li, W., Li, R., Li, Y., & Wang, G. (2018). Mitigation effect of waste glass powders on alkali-silica reaction expansion in cementitious composite. *International Journal of Concrete Structures and Materials*, *12*, 1-14.

Kou, S.C., & Poon, C.S. (2020). Effect of different recycled aggregates on rendering mortar.

Lalit, K.G., & Ashok, K.V. (2021). Impact on mechanical properties of cement fine aggregate mortar containing waste granite powder.

Li, Q., Qiao, H., Li, A., & Li, G. (2022). Performance of waste glass powder as pozzolanic material in cement mortar. *Construction and Building Materials*, *324*, 126531.

Mobasher, B., Devaguptapu, R., & Arino, A.M. (1996). Effect of copper slag on the hydration of blended cementitious mixtures. In *Materials for the New Millennium: Proceedings of ASCE Materials Engineering Conference*, ASCE.

Moghaddas, S.A., Nekoei, M., Golafshani, E.M., Nehdi, M., & Arashpour, M. (2022). Modeling carbonation depth of recycled aggregate concrete using automatic regression. *Journal of Cleaner Production*, *371*, 133522.

Ramadoss, P., & Sundararajan, T. (2014). Lignite bottom ash as partial replacement of fine aggregate in masonry mortar. *Arabian Journal for Science and Engineering*, *39*, 737-745.

RILEM. (1988). *RILEM CPC-18: Measurement of hardened concrete carbonation depth.*

Saiz Martinez, P., Gonzalez Cortina, M., Fernandez, F., & Rodriguez Sanchez, A. (2017). Comparative study of three types of fine recycled aggregates for masonry. *(Incomplete citation)*

Salahaddin, S.D., Haido, J.H., & Wardeh, G. (2024). Basalt fiber UHPC with waste glass powder replacing cement. *Ain Shams Engineering Journal*, *15*(3), 102515.

Saranya, P., Nagarajan, P., & Shashikala, A.P. (2021). Engineering and durability properties of slag-dolomite geopolymer mortars. *Proceedings of the Institution of Civil Engineers - Construction Materials*. https://doi.org/10.1680/jcoma.18.00096

Sivasakthi, M., Jeyalakshmi, R., & Rajamane, N.P. (2021). Fly ash geopolymer mortar with copper slag as fine aggregate: Thermal resistance. *Journal of Cleaner Production*, *279*, 123766.

Soriano, L., Monzó, J., Bonilla, M., Tashima, M.M., Payá, J., & Borrachero, M.V. (2013). Effect of pozzolans on hydration of Portland cement at low temperatures. *Cement and Concrete Composites*, *42*, 41-48.

Sreenivasulu, C., Jawahar, J.G., & Sashidhar, C. (2020). Effect of copper slag on micro, macro, and flexural characteristics of geopolymer concrete. *Journal of Materials in Civil Engineering*, *32*, 04020086. https://doi.org/10.1061/(ASCE)MT.1943-5533.0003 157

Srinivasreddy, K., Bala Murugan, S., Jindal, B. B., & Vali, K.S. (2022). Experimental study on ternary blended geopolymer-rich mortar. *Innovative Infrastructure Solutions*, *7*, 1-9. https://doi.org/10.1007/s41062-022-00757-4

Swanepoel, C.A.S.J.C. (2002). Utilisation of fly ash in a geopolymeric material. *Applied Geochemistry*, *17*, 1143-1148. https://doi.org/10.1016/S0883-2927(02) 00005-7

Tironi, A., Trezza, M. A., Irassar, E. F., & Scian, A. N. (2012). Thermal treatment of kaolin: Effect on the pozzolanic activity. *Procedia Materials Science*, *1*, 343-350. https://doi.org/10.1016/j.mspro.2012.06.046

Wang, T., San Nicolas, R., Nguyen, T.N., Kashani, A., & Ngo, T. (2023). Long-term ASR expansion in mortar with recycled glass. *Cement and Concrete Composites*, *139*, 105043.

Xu, J., Zhan, P., Zhou, W., Zuo, J., Shah, S. P., & He, Z. (2023). Design and assessment of eco-friendly UHPC with steel slag powder and recycled glass powder. *Powder Technology*, *419*, 118356.

Xu, Z., Yue, J., Pang, G., Li, R., Zhang, P., & Xu, S. (2021). Strength and shrinkage of alkali-activated slag geopolymer pastes. *Advances in Civil Engineering*, *2021*. https://doi.org/10.1155/2021/6631316

Zhang, X., Tang, Z., & Ke, G., Li, W. (2021). Mechanical properties and durability of concrete with industrial solid wastes. *Transportation Research Record*, *2675*(12), 797-810.